Molecular-Level Simulations of Turbulence and Its Decay

M. A. Gallis,[1,*] N. P. Bitter,[1] T. P. Koehler,[1] J. R. Torczynski,[1] S. J. Plimpton,[2] and G. Papadakis[3]

[1]*Engineering Sciences Center, Sandia National Laboratories, P.O. Box 5800, Albuquerque, New Mexico 87185-0840, USA*
[2]*Computing Research Center, Sandia National Laboratories, P.O. Box 5800, Albuquerque, New Mexico 87185-1316, USA*
[3]*Department of Aeronautics, Imperial College, London SW7 2AZ, United Kingdom*

We provide the first demonstration that molecular-level methods based on gas kinetic theory and molecular chaos can simulate turbulence and its decay. The direct simulation Monte Carlo (DSMC) method, a molecular-level technique for simulating gas flows that resolves phenomena from molecular to hydrodynamic (continuum) length scales, is applied to simulate the Taylor-Green vortex flow. The DSMC simulations reproduce the Kolmogorov $-5/3$ law and agree well with the turbulent kinetic energy and energy dissipation rate obtained from direct numerical simulation of the Navier-Stokes equations using a spectral method. This agreement provides strong evidence that molecular-level methods for gases can be used to investigate turbulent flows quantitatively.

Turbulence is almost exclusively studied at the hydrodynamic (continuum) level. Molecular-level simulations of turbulence have received little, if any, attention to date because the molecular scales and the turbulent scales are considered to be many orders of magnitude apart, and, as a result, molecular turbulence simulations have been heretofore considered to be physically unnecessary and computationally intractable. However, there are cases of practical interest in which the Kolmogorov length and time scales, which are the smallest length and time scales in a turbulent flow, can be within 1–2 orders of magnitude of the mean free path and the mean collision time. For a high-speed gas flow with a turbulent Mach number M and a turbulent Reynolds number Re, the ratio of the Kolmogorov length scale to the mean free path scales as $\mathrm{Re}^{1/4}/M$, and the ratio of the Kolmogorov time scale to the mean collision time scales as $\mathrm{Re}^{1/2}/M^2$ [1]. Thus, for $M = 1$ and Re = 10000, these ratios are ~10 and ~100, respectively. In such cases, studying turbulence and energy exchange at the molecular level may offer new physical insights.

The most common starting point for any molecular-level, kinetic-theory investigation of a gas flow is the Boltzmann equation (BE). Kinetic theory describes a gas in terms of a distribution function f of molecular velocities and positions. The velocity distribution function f provides a complete description of a dilute monatomic gas at the molecular level. The BE gives the evolution of the velocity distribution function f:

$$\frac{\partial}{\partial t}(nf) + \mathbf{v}\cdot\frac{\partial}{\partial \mathbf{x}}(nf) + \frac{\mathbf{F}}{m}\cdot\frac{\partial}{\partial \mathbf{v}}(nf)$$
$$= \int_{-\infty}^{\infty}\int_{0}^{4\pi} n^2(f^* f_1^* - f f_1)c_r\sigma d\Omega d\mathbf{v}_1, \quad (1)$$

where t is the time, $\mathbf{x}$ is the position in physical space, $\mathbf{v}$ is the molecular velocity, $\mathbf{F}$ is any external force (velocity-independent above and zero herein), m is the molecular mass, and n is the number density. The right side is the collision integral. In this integral, the distribution functions f and f^* are evaluated at the molecule's precollision velocity $\mathbf{v}$ and postcollision velocity $\mathbf{v}^*$, respectively, and the distribution functions f_1 and f_1^* are evaluated at the collision partner's precollision velocity $\mathbf{v}_1$ and postcollision velocity $\mathbf{v}_1^*$, respectively. Also in the collision term, $c_r = |\mathbf{v} - \mathbf{v}_1|$ is the relative speed of the colliding molecules, σ is the cross section of the binary collision, and Ω is the solid angle. The details of the binary collision are included in the collision cross section.

The BE is based on two fundamental assumptions. The first is that only binary collisions are considered. The second is that molecular chaos applies (the "Stosszahlansatz"), which leads to the time irreversibility of the BE. The apparent incompatibility between the irreversible tendency of the BE velocity distribution function toward equilibrium and the underlying reversibility of molecular collisions suggests a stochastic interpretation of the BE velocity distribution function as the most probable number of molecules at a particular point in phase space [2]. Aristov [3] and Tsugé [4] suggest that the introduction of fluctuations into the BE is critical for simulating turbulent flows. Tsugé [4] further argues that the BE could simulate turbulent flows if the BE velocity distribution function were replaced by a particle-based distribution function like the Klimontovich distribution function f_K:

$$f_K(\mathbf{x}, \mathbf{v}, t) = \sum_{i=0}^{N} \delta^3(\mathbf{x} - \mathbf{x}_i(t))\delta^3(\mathbf{v} - \mathbf{v}_i(t)). \quad (2)$$

In this approach, the ensemble average of f_K is the distribution function f that appears in the BE. Thus, a

particle-based distribution function provides microscopic detail not available to the BE distribution function, in the sense that it allows the appearance of fluctuations, which are otherwise absent from the BE. Moreover, Grad [5] showed that uncorrelated initial conditions are the most probable initial conditions for molecule collisions. This observation suggests that the assumption of molecular chaos at the microscopic level does not preclude the establishment of fluctuations at the macroscopic level [3,6].

Thus, the ability of the BE to simulate turbulent flows has been suggested theoretically [3,4,6] but has not yet been investigated computationally. The major problem is the magnitude of the computational effort required to resolve all of the length scales from the molecular to the macroscopic. High-performance computing platforms have only recently become available on which molecular-level gas-flow simulations resolving turbulent length scales are possible, albeit computationally intensive.

Bird's direct simulation Monte Carlo (DSMC) method [7] is widely used as a surrogate for a direct solution of the BE. DSMC is a molecular-level technique for simulating gas flows when the mean free path is much larger than the molecular diameter, which is typically the case. DSMC uses a molecular-level, stochastic algorithm that approximates the continuous velocity distribution function of the BE with a discrete number of computational molecules or "particles," just as in the Klimontovich distribution function in Eq. (2). Each of the N particles typically represents a large number of real molecules, and these particles move, collide with other particles, and reflect from boundaries just as real molecules do. Substituting Eq. (2) into Eq. (1) yields $2N$ differential equations [8]:

$$d\mathbf{x}_i/dt = \mathbf{v}_i, \qquad d(m_i\mathbf{v}_i)/dt = \mathbf{F}(\mathbf{x}_i) + \mathbf{C}(\mathbf{v}_i), \quad (3)$$

where $\mathbf{C}(\mathbf{v}_i)$ represents the binary collision process each particle undergoes during the time step and $\mathbf{F}(\mathbf{x}_i)$ is the external force (zero herein).

The physical domain is discretized into a set of cells. A time-splitting scheme based on Eq. (3) is used that consists of a move operation, during which particles translate ballistically over time step Δt, followed by a collide operation, during which pairs of particles within the same cell are randomly selected for collision. Unlike the Klimontovich distribution, in which particles are mathematical points in space, particles are assigned finite collision cross sections based on the intermolecular interaction of interest. Macroscopic gas properties are determined by sampling the properties of the particles resident in a cell at a particular time. Standard DSMC executes each of these operations once per time step in the order move-collide-sample.

Wagner [9] proved that DSMC simulations approach solutions of the BE for monatomic molecules in the limit of vanishing discretization and statistical errors. Gallis,

Torczynski, and Rader [10] reported DSMC results for transport properties and velocity distribution functions that are in excellent agreement with Chapman-Enskog infinite-approximation results [11] for conditions that are near equilibrium and with moment-hierarchy results for conditions that are far from equilibrium [12].

DSMC inherently accounts for both near-equilibrium transport (viscosity, thermal conductivity, and mass diffusivity) and nonequilibrium phenomena (thermal and pressure diffusion) [6]. More importantly, DSMC inherently reproduces the thermal fluctuations that in some cases may trigger the instabilities leading to coherent flow structures and turbulence [13,14]. When each particle represents a single actual molecule, DSMC exactly reproduces the fluctuations in an equilibrium gas [13], which are typically extremely small. When each particle represents many actual molecules, the variances of the fluctuations in a DSMC simulation are the actual variances multiplied by the number of actual molecules represented by each particle (i.e., the simulation ratio). In this situation, these fluctuations can be reduced to an acceptable level, relative to macroscopic velocities, through ensemble averaging [15].

The substantial computational effort needed to achieve acceptable signal-to-noise ratios for high-density, low-speed flows has generally prevented DSMC and other molecular-level methods from simulating macroscopic hydrodynamic (continuum) phenomena at the molecular level. Recently, however, DSMC simulations of the Richtmyer-Meshkov and Rayleigh-Taylor instabilities have been successfully performed using massively parallel computers [14,15]. To demonstrate the ability of DSMC to simulate turbulent flows, simulations of the Taylor-Green (TG) vortex flow [16] are performed. TG flow is a canonical turbulent flow in which the generation of small-scale eddies and the corresponding cascade of energy from small to large wave numbers can be numerically observed. TG flow has been used extensively to study isotropic turbulence [17–19]. TG flow is initialized in a triply periodic domain $-\pi L \leq \mathbf{x} \leq \pi L$ using a flow field that contains only a single length scale L and a single velocity scale V_0:

$$u = V_0 \sin(x/L)\cos(y/L)\cos(z/L),$$
$$v = -V_0 \cos(x/L)\sin(y/L)\cos(z/L),$$
$$w = 0,$$
$$p = p_0 + \frac{\rho_0 V_0^2}{16}[\cos(2x/L) + \cos(2y/L)]$$
$$\times [\cos(2z/L) + 2], \quad (4)$$

where $\mathbf{u} = (u, v, w)$ is the flow velocity and p is the pressure at position $\mathbf{x} = (x, y, z)$. Thus, all of the kinetic energy in the flow is initially resident in a single wave number.

The evolution of TG flow is described in terms of the nondimensional time $T = V_0 t/L$. Early on, the flow is highly anisotropic and laminar. Nonlinear interactions between the developing eddies result in an energy cascade from small to large wave numbers and the rapid development of a turbulent spectrum. Later on, a catastrophic collapse of the accumulated energy leads the flow to a state that exhibits features of isotropic, homogeneous turbulence [17]. An important mechanism involved in homogeneous three-dimensional turbulent flows is the maintenance and enhancement of vorticity by vortex-line stretching and the consequent production of small-scale eddies [1]. This process controls the turbulent-energy dynamics and hence the global structure and evolution of the flow [18].

The rate at which energy dissipates to larger wave numbers is a weak function of the Reynolds number. Increasing the Reynolds number from 400 to 5000 increases the maximum dissipation rate by only 40% [18]. However, for Re $\leq$ 400, the maximum dissipation is achieved at approximately the same time ($T = 5$), whereas for Re $\geq$ 500, a second maximum in the dissipation appears at a later time ($T = 9$). As a result, in the range of $400 \leq \text{Re} \leq 500$, the dissipation rate has an extended region over which near-maximum dissipation is observed.

The DSMC code SPARTA [20,21] was used to simulate TG flow at Re $= 450$ to obtain quantitative results for the energy dissipation rate and the spectral energy distribution. These simulations were performed on Sequoia, an IBM Blue Gene/Q supercomputer at Lawrence Livermore National Laboratory, and used more than half a million cores for 500 h. The simulation domain is a triply periodic cube with sides of length $2\pi L$, where $L = 0.0001$ m. The gas is taken to have the molecular mass of nitrogen, and the initial density and temperature correspond to values at STP (101 325 Pa and 273.15 K, respectively). The simulations used 8 billion cells (2000^3) and an average of 30 particles per cell for a total of 0.24 trillion particles. To improve the spatial discretization, collision partners are selected from within a sphere having a radius that equals the distance traveled by the particle during a time step. The characteristic (maximum) velocity V_0 corresponds to a Mach number of 0.3, so the simulation conditions marginally satisfy the incompressibility assumption (less than 8% maximum error) [22]. Molecular collisions are performed using the variable soft sphere collision model [6], which for nitrogen produces a viscosity with a $T_{\text{thermal}}^{0.74}$ dependence on the thermal temperature T_{thermal}. Multiple collisions between the same molecules during the same time step are not allowed, which enforces molecular chaos in the collision process.

The discretization errors in DSMC act to increase the transport properties [23]. For these simulations, the effective viscosity and hence the effective Reynolds number are determined by comparing a thin-slab DSMC simulation (one layer of cells in the z direction) of the two-dimensional

TG flow to the analytical expression for the decay of its kinetic energy [19]. This comparison indicates that the particular discretization used for these simulations leads to an effective Reynolds number of Re $= 450$. For these conditions, the ratio of the Kolmogorov length scale to the mean free path is about 15, and the ratio of the Kolmogorov time scale to the mean collision time is about 235, which suggests that molecular effects play at most a small role, even for the smallest scales.

The direct numerical simulation (DNS) simulations to which the DSMC simulations are compared were carried out using the spectral element code NEK5000 [24]. The simulation domain was a cube with sides of length 2π, and the initial conditions given by Eq. (4) are imposed using a characteristic velocity $V_0 = 1$. The fluid is modeled as incompressible with a constant viscosity of $\mu = 1/\text{Re}$ and a constant density of $\rho = 1$. It is noted that, since the total temperature increase is less than 2 K, this is a reasonable assumption. The simulation domain was discretized using 32 seventh-order spectral elements along each coordinate direction. Each spectral element contained 8^3 grid points placed at the Gauss-Lobatto nodes, for a total of 256 grid points along each coordinate axis. Third-order-accurate temporal integration is employed with a fixed Courant number of 0.8. After the simulation, the velocity fields are interpolated onto a uniform grid using the seventh-order polynomials associated with the spectral elements as interpolants. After interpolating the data onto this grid of equally spaced points, discrete Fourier transforms are applied to obtain the energy spectra. To verify the DNS approach, the TG simulations of van Rees [25] at a Reynolds number of Re $= 1600$ are reproduced. To confirm that the results reported here are mesh independent, simulations are performed on 256^3 and 512^3 grids (i.e., 32 and 64 elements along each coordinate axis). The dissipation rates are found to differ by only 0.02% at $T = 9$ and by at most only 0.06% over $0 \leq T \leq 20$.

Figures 1 and 2 present the u velocity component on the bounding planes of the domain from the DNS and DSMC simulations at $T = 9$, the time of maximum dissipation, and at $T = 20$. Except for being slightly noisy, the DSMC molecular results are virtually identical to the DNS Navier-Stokes results at both times. A detailed presentation of the evolution of the flow field can be found in the works of Brachet *et al.* [17] and Canuto *et al.* [19]. At the time of maximum dissipation, the large-scale structures that are the remnants of the initial conditions are still discernible, but many smaller-scale structures are also present. This behavior is in good qualitative agreement with previously published results [19]. At $T = 20$, the original structures have become much weaker because the flow field has almost thermalized.

Figure 3 presents the turbulent-kinetic-energy decay as a function of time. The DSMC results are seen to agree closely with the DNS results over the entire time period
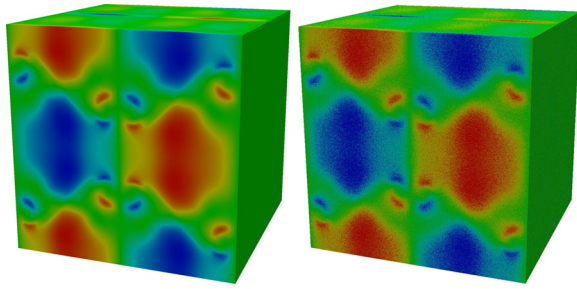
FIG. 1.   DNS (left) and DSMC (right) plots of the u velocity at $T = 9$, the time of maximum dissipation.

except at late times after most of the kinetic energy has decayed and with the theory of Taylor and Green [16] at early times. The DSMC and DNS results are both normalized by their initial values, and the DSMC results are averaged over a window of $\Delta T = 0.3$ to reduce statistical noise. Since the theory of Taylor and Green is accurate only for $T \leq 3$ [16], results from this theory are presented only up to $T = 3$. Kinetic energy is ultimately converted to thermal energy through molecular collisions (viscosity). For $T < 3$, the rate of conversion is slow. At $T = 3$, beyond which the theory of Taylor and Green becomes inaccurate, the rate increases. The rapid conversion of kinetic energy to thermal energy between $T = 5$ and $T = 12$ is captured equally well by both simulations. After $T = 12$, the rate of conversion decreases because most of the kinetic energy has decayed. This observation is in agreement with the assertions that the early stages of TG flow are driven mainly by inertial subrange physics and that the later stages are determined mainly by the viscosity [17].

Figure 4 presents the energy dissipation rate as a function of time. The DSMC and DNS results are in good agreement over the entire time period during which the energy dissipation rate is significant. Both methods yield the same rapid increase from $T = 2$ to $T = 6$, the same plateau from $T = 6$ to $T = 8$, the same maximum between $T = 8$ and $T = 9$, the same rapid decrease from $T = 9$ to $T = 15$, and the same slow decrease from $T = 15$ to $T = 20$. In accord with Fig. 2, DSMC does generally yield a slightly faster rate than DNS (the noticeably larger rate for $T \leq 2$ may be caused by compressibility effects related to the finite initial
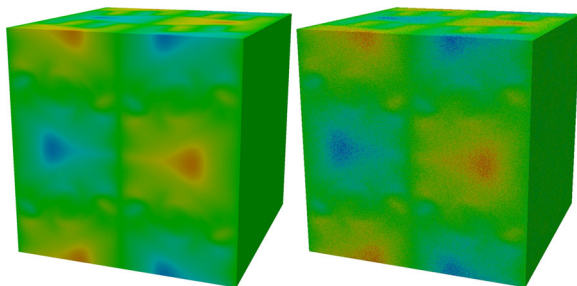

FIG. 2.   DNS (left) and DSMC (right) plots of the u velocity at $T = 20$.
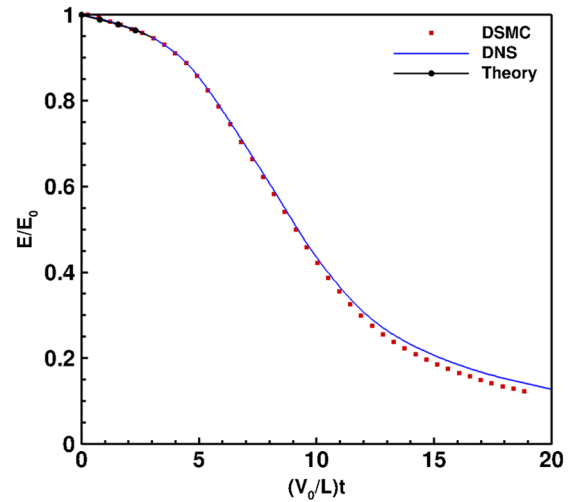

FIG. 3.   Turbulent-kinetic-energy decay as a function of time.

Mach number, 0.3). Results from the viscous theory of Taylor and Green [16] and from the inviscid theory by Brachet *et al.* [17] are also shown in this figure. Both theories are valid only for early times ($T < 3$ and $T < 4$, respectively). For $T > 2$, these two approximate theories bracket the DSMC and DNS results.

Figure 5 presents three-dimensional kinetic-energy spectra at times near maximum dissipation. The DSMC spectra from $T = 7.5$ to $T = 9$ and the DNS spectrum at $T = 9$ are in good agreement and all exhibit the Kolmogorov $-5/3$ law over about 70% of a decade. As time progresses, the energy in the low-wave-number, large-wavelength region of the spectrum decreases. During this time, energy is transferred from the initial large wavelength to smaller wavelengths, a process known as the energy cascade.

The fact that the DSMC results agree closely with the DNS results, the theory of Taylor and Green, and the theory of Kolmogorov suggests that DSMC can be used for quantitative investigations of turbulence and its decay.
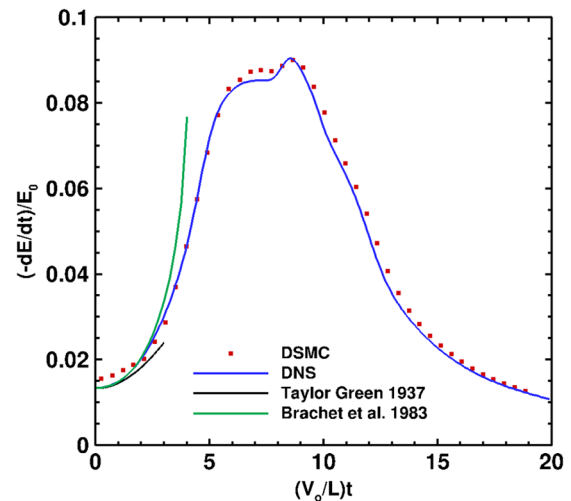

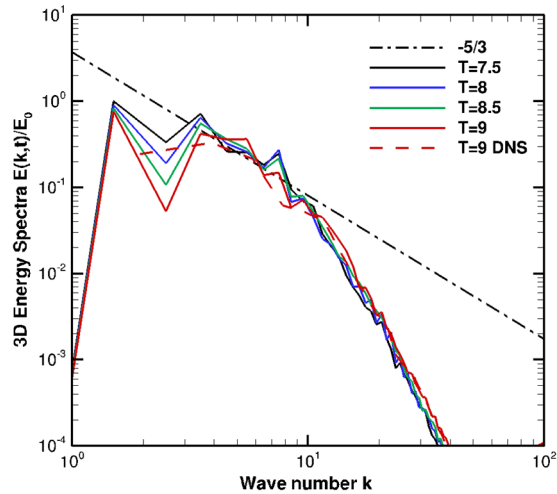FIG. 4.   Energy dissipation rate as a function of time.

FIG. 5.   Three-dimensional kinetic-energy spectra at times near maximum dissipation.

This observation is in agreement with the theoretically based suggestions of Aristov [3] and Tsugé [4] about the ability of the BE and molecular-level methods to simulate turbulent flows. In this sense, DSMC can be viewed as an extension of DNS methods in that the subcell dissipative processes are inherently represented without filtering out naturally occurring thermodynamic fluctuations. Although molecular fluctuations may well affect the transition to turbulence [15], they do not affect the decay of turbulence significantly for the Taylor-Green vortex flow studied herein and presumably for other similar flows. Thus, taking advantage of ever-increasing computer power, DSMC offers the possibility of generating molecular-level data sets that complement existing computational and experimental data sets, especially for realistic flight geometries in hypersonic flows.

Since it inherently represents molecular-level effects and thermal fluctuations, DSMC has the potential to improve our understanding of how these phenomena influence turbulence. In DSMC, hydrodynamic quantities such as compressibility, viscosity, thermal conductivity, and diffusivity arise directly from molecular processes, so their effects on turbulence are automatically captured. Since internal energy modes (rotation and vibration) and chemical reactions are also represented at the molecular level, DSMC offers a natural way to study their effects on turbulence. Moreover, the effect of surface roughness on wall-bounded turbulence can be investigated fundamentally because DSMC treats gas-wall interactions at the molecular level.

* magalli@sandia.gov

 [1] H. Tennekes and J. L. Lumley, *A First Course in Turbulence* (MIT Press, Cambridge, MA, 1972).
 [2] V. Garzó and A. Santos, *Kinetic Theory of Gases in Shear Flows* (Kluwer Academic, Dordrecht, 2003).
 [3] V. V. Aristov, *Direct Methods for Solving the Boltzmann Equation and Study of Nonequilibrium Flows* (Springer, New York, 2001).
 [4] S. Tsugé, Phys. Fluids **17**, 22 (1974).
 [5] H. Grad, J. Chem. Phys. **33**, 1342 (1960).
 [6] M. N. Kogan, *Rarefied Gas Dynamics* (Plenum, New York, 1969).
 [7] G. A. Bird, *Molecular Gas Dynamics and the Direct Simulation of Gas Flows* (Clarendon, Oxford, 1998).
 [8] I. Sagert, W. Bauer, D. Colbry, J. Howell, R. Pickett, A. Staber, and T. Strother, J. Comput. Phys. **266**, 191 (2014).
 [9] W. Wagner, J. Stat. Phys. **66**, 1011 (1992).
[10] M. A. Gallis, J. R. Torczynski, and D. J. Rader, Phys. Rev. E **69**, 042201 (2004).
[11] S. Chapman and T. G. Cowling, *The Mathematical Theory of Non-Uniform Gases*, third ed. (Cambridge University Press, Cambridge, England, 1970).
[12] M. A. Gallis, J. R. Torczynski, D. J. Rader, M. Tij, and A. Santos, Phys. Fluids **18**, 017104 (2006).
[13] A. L. Garcia, Phys. Rev. A **34**, 1454 (1986).
[14] M. A. Gallis, T. P. Koehler, J. R. Torczynski, and S. J. Plimpton, Phys. Fluids **27**, 084105 (2015).
[15] M. A. Gallis, T. P. Koehler, J. R. Torczynski, and S. J. Plimpton, Phys. Rev. Fluids **1**, 043403 (2016).
[16] G. I. Taylor and A. E. Green, Proc. R. Soc. A **158**, 499 (1937).
[17] M. E. Brachet, D. I. Meiron, S. A. Orszag, B. G. Nickel, R. H. Morf, and U. Frisch, J. Fluid Mech. **130**, 411 (1983).
[18] U. Frisch, *Turbulence: The Legacy of A. N. Kolmogorov* (Cambridge University Press, Cambridge, England, 1996).
[19] C. Canuto, M. Y. Hussaini, A. Quarteroni, and T. A. Zang, *Spectral Methods: Evolution to Complex Geometries and Applications to Fluid Dynamics* (Springer, New York, 2007).
[20] S. J. Plimpton and M. A. Gallis, http://sparta.sandia.gov.
[21] M. A. Gallis, J. R. Torczynski, S. J. Plimpton, D. J. Rader, and T. Koehler, *AIP Conf. Proc.* 1628, 27 (2014).
[22] A. J. Smits, *A Physical Introduction to Fluid Mechanics* (Wiley, New York, 1999).
[23] D. J. Rader, M. A. Gallis, J. R. Torczynski, and W. Wagner, Phys. Fluids **18**, 077102 (2006).
[24] P. F. Fischer and J. W. Lottes, in *Domain Decomposition Methods in Science, and Engineering, Lecture Notes in Computational Science, and Engineering Vol.* 40, edited by T. J. Barth *et al.* (Springer, Berlin, 2005).
[25] W. M. van Rees, A. Leonard, D. I. Pullin, and P. Koumoutsakos, J. Comput. Phys. **230**, 2794 (2011).